

See discussions, stats, and author profiles for this publication at: <https://www.researchgate.net/publication/282432888>

Defects in zinc oxide grown by pulsed laser deposition

Article in *Physica B Condensed Matter* · September 2015

DOI: 10.1016/j.physb.2015.09.034

CITATIONS

0

READS

146

8 authors, including:



Muhammad Younas

The University of Hong Kong

14 PUBLICATIONS 201 CITATIONS

[SEE PROFILE](#)



Wolfgang Anwand

Helmholtz-Zentrum Dresden-Rossendorf

253 PUBLICATIONS 2,320 CITATIONS

[SEE PROFILE](#)



Andreas Wagner

Helmholtz-Zentrum Dresden-Rossendorf

283 PUBLICATIONS 4,232 CITATIONS

[SEE PROFILE](#)



Chong-Xin Shan

Chinese Academy of Sciences

187 PUBLICATIONS 3,368 CITATIONS

[SEE PROFILE](#)

Some of the authors of this publication are also working on these related projects:



nELBE neutron time-of-flight [View project](#)



radiation effects [View project](#)

All content following this page was uploaded by [Chi-Chung Ling](#) on 06 November 2015.

The user has requested enhancement of the downloaded file. All in-text references [underlined in blue](#) are added to the original document and are linked to publications on ResearchGate, letting you access and read them immediately.

Defects in Zinc Oxide Grown By Pulsed Laser Deposition

Francis C. C. Ling*, Zilan Wang, Lok Ping Ho, M. Younas
*Department of Physics, The University of Hong Kong, Pokfulam Road, Hong Kong,
P. C. China*

W. Anwand, A. Wagner,
*Institute of Radiation Physics, Helmholtz-Zentrum Dresden-Rossendorf, Bautzner
Landstr. 400, 01328 Dresden, Germany*

S. C. Su
*Institute of Optoelectronic Material and Technology, South China Normal University,
Guangzhou 510631, P. R. China*

C. X. Shan
*State Key Laboratory of Luminescence and Applications, Changchun Institute of
Optics, Fine Mechanics and Physics, Chinese Academy of Sciences, Changchun
130033, China*

* E-mail of contact author: ccling@hku.hk

ZnO films are grown on c-plane sapphire using the pulsed laser deposition method. Systematic studies on the effects of annealing are performed to understand the thermal evolutions of the defects in the films. Particular attention is paid to the discussions of the ZnO/sapphire interface thermal stability, the Zn-vacancy related defects having different microstructures, the origins of the green luminescence (~2.4-2.5 eV) and the near band edge (NBE) emission at 3.23 eV.

Introduction

Zinc oxide is a semiconductor having a direct band gap of 3.3 eV at 300 K and a large exciton binding energy of ~ 60 meV. It has received extensive attention because of its potential in a variety of applications including ultra-violet (UV) optoelectronics, photovoltaics, sensors, and spintronics etc [1]. As compared to GaN, which is more maturely developed for optoelectronic device applications, ZnO has the advantage of its large exciton binding energy (~ 60 meV). Excitons in ZnO are thermally stable at room temperature, thus enabling intense near band edge (NBE) exciton emission and low threshold lasing at room temperature [2].

Despite its potential in fabricating UV optoelectronic devices with good performance, the realization of practical ZnO-based devices is hindered by the asymmetric p-type doping difficulty of ZnO [1, 3-4]. Defects in ZnO play a crucial role in determining the electrical, optical and magnetic properties of the material and thus the devices. However, the knowledge of defects in ZnO is far from complete [5].

The present paper reports our recent work on studying the defects in ZnO films grown by the pulsed laser deposition (PLD) method using a comprehensive spectroscopic approach. These include a summary of our recently published works in references [6] and [7], as well as some unpublished new results of the research in progress.

EXPERIMENTAL

Undoped ZnO films having thickness of 300 nm were grown on c-sapphire substrate using the PLD method and a ZnO target with purity of 99.999%. To obtain comprehensive results, the films were grown with different substrate temperatures ($T_{\text{sub}}=300$ and 600°C) and oxygen pressures ($P(\text{O}_2)=0, 1.3$ and 5 Pa) systematically.

Cu-doped ZnO samples were also grown on c-sapphire with $T_{\text{sub}}=600^{\circ}\text{C}$ and $P(\text{O}_2)=0$ using a ZnO:CuO target with a weight ratio of 99%:1%. Isochronal annealing was performed in Ar atmosphere for 40 minutes with two approaches being adopted, namely (i) with another piece of ZnO placed on top to protect the sample surface during the annealing, and (ii) the sample being annealed is exposed to the Ar atmosphere without coverage. To obtain a comprehensive picture of the defects in the samples, a multi-spectroscopic approach was adopted to characterize the samples. These included X-ray diffraction (XRD), atomic force microscopy (AFM), high resolution transmission electron microscopy (HRTEM), secondary ion mass spectroscopy (SIMS), photoluminescence (PL), and positron annihilation spectroscopy (PAS). We have studied the effect of whether the sample surface was covered by another piece of ZnO. Experimental detail concerning the growth, post-growth annealing and the spectroscopic characterizations are given in references [6] and [7].

RESULTS AND DISCUSSION

The ZnO films exhibit only the (002) and (004) peaks in the XRD spectra. The films have electron concentrations of 1×10^{18} to $2 \times 10^{19} \text{ cm}^{-3}$ and the mobility varies from 25 to $95 \text{ cm}^2 \text{V}^{-1} \text{s}^{-1}$ depending on T_{sub} and $P(\text{O}_2)$ during growth, as well as the post-growth annealing temperature [6].

Atomic force microscopy (AFM) studies [6] showed that the surface roughness of the as-grown undoped film grown without oxygen is 1.97 nm. The surface morphology upon annealing at 900°C is dependent on whether the sample surface is covered during annealing. The uncovered annealing introduces surface

damage and the surface roughness increases to 3.37 nm. For the covered annealing, the surface roughness is improved to 0.82 nm.

Whether the sample surface is covered during annealing also influences the thermal stability of the ZnO/sapphire interface. The HRTEM images of the undoped samples grown at $T_{\text{sub}}=600\text{ }^{\circ}\text{C}$ and $P(\text{O}_2)=0\text{ Pa}$ upon annealing at $750\text{ }^{\circ}\text{C}$ without and with the cover are shown in figure 1(a) and (b) respectively. The HRTEM image of the sample annealed without coverage (figure 1(a)) shows perfect ZnO growth along (002) plane and the interface to be atomically sharp (parallel lattice fringes can be seen even very close to the interface) without any interfacial reactions and inter-diffusion. The film/substrate shows clear continuity without bending and wrinkling of the lattice fringes. The diffraction pattern from film-substrate interface (inset of Fig.1(a)) shows perfect epitaxial growth and the absence of spots apart from those belonging to the film and substrate. The native ZnO film also demonstrates some image contrast (dark and white regions) revealing non-uniform density distribution due to introduction of some intrinsic defects after annealing. Similarly Fig.1(b) demonstrates a cross-sectional HRTEM image at the film/substrate interface for the sample annealed with cover. The image shows perfect ZnO growth along the (002) plane but the film/substrate interface is not atomically sharp as that observed in the previous case. We can see atomically thick and crumpled film/substrate interface and clear discontinuity at some localized region (marked by circle). This discontinuity may possibly arise because of localized interfacial reactions due to Zn out-diffusion into the substrate. Moreover, the native ZnO thin film show less image contrast indicating more uniform density distribution due to suppression of intrinsic defects but at the expense of deterioration of film/substrate interface.

The Zn and Al profiles obtained by secondary ion mass spectroscopy (SIMS)

of the undoped ZnO samples annealed at 900 °C with and without coverage are shown in figure 2(a) and (b). The figures show that the Zn out-diffusion of the sample annealed with cover is more extensive than that without the cover, which agrees with the speculation made in the last paragraph that the discontinuity observed in the HRTEM image of the interface is due to Zn out-diffusion, which would be enhanced by the coverage during the annealing. The out-diffusion of Zn at the interface could lead to the formation of Zn-vacancy related defects. The Al out-diffusion is similar for the two samples annealed with and without the coverage.

Low temperature (LT) PL study was carried out to study the defects in ZnO samples annealed at different temperatures with coverage [7]. Broad defect emissions peaking at 2.2 eV to 2.5 eV are found in the low temperature (10 K) PL spectra of the undoped samples, with the peak positions and shapes depending on the growth parameters and the subsequent annealing temperature. However, irrespective of the initial growth parameter, after post-growth annealing at 900°C with the surface covered, all the undoped samples exhibit an identical green luminescence having the same peak position (2.47 eV) and shape (see the normalized spectra in the insert of figure 3(a)). The defect emissions of the samples annealed at temperatures lower than 900°C originate from more than one defect. The relative compositions of the defects are dependent on the annealing temperature and the initial growth conditions, and thus so are the shape and the peak of the resultant defect emission spectra. After the 900°C annealing, all the samples irrespective of the initial growth condition exhibit the same GL peaking at 2.47 eV (GL-2.47eV), which is interpreted as that the GL originates from a single type of defect and that the other defects contributing to the defect emission have already been thermally removed (with the spectrum shown in figure 3(a)). The GL disappears after annealing at 1100 °C.

For the 10 K NBE emission spectra of the undoped as-grown samples, the neutral bound exciton (D^0X) emission at ~ 3.356 eV, as well as its 1LO and 2LO are observed [7]. The D^0X emission persists after the annealing at 900°C (as shown in figure 3(b)). Moreover after the annealing at 900°C , emission at 3.229 eV and its first and second phonon replicas (1LO and 2LO) are introduced (figure 3(b)). These three peaks blue-shift with the increasing measuring temperature (see figure 3(b)), and are associated to the combined contributions from the transitions of donor-acceptor-pair (DAP) and the free-electron-to-acceptor (FA).

The defect emission of the undoped sample (grown with no oxygen and the substrate temperature of 300°C) annealed at 900°C without cover is shown in figure 3(a). This spectrum (denoted by GL-FS) has the peak at 2.42 eV and has the fine structured peaks separated by ~ 70 meV, which coincides with the LO phonon energy of ZnO. The same defect emission is also found in the Cu-doped ZnO samples annealed at 900°C with cover (spectrum shown in figure 3(a)) and without cover. The GL-FS defect emission is clearly not the same type of the defect emission GL-2.47eV. Dingle [8] has observed a similar GL with fine structure and attributed it to be Cu-impurity related. With illumination, Cu^{2+} substituting the Zn site would receive an electron from the neighboring O, and become the transient shallow acceptor state (Cu^+ , h) consisting of the Cu^+ and a hole (references in review [5]). The green luminescence is attributed to the transition from the (Cu^+ , h) shallow acceptor state to the $\epsilon(0/-)$ state of the Cu_{Zn} acceptor (i.e. the T_2 state) having the zero phonon line at 2.86 eV (references in review [5]). The fine structured small peaks have been attributed to the strong coupling between the electronic transition and the LO phonon [5]. The mechanism for introducing the GL-FS in the undoped sample annealed at 900°C without cover is still unknown and study is in progress.

Positron annihilation spectroscopy (PAS) is a non-destructive probe for characterizing vacancy type defects in semiconductors [9,10]. The Doppler broadening of the annihilation spectrum is monitored by the S and the W parameters. For the case of ZnO, PAS is selectively sensitive to V_{Zn} -related defects at the room temperature measurement. Our recent S-W parameter study of the samples annealed at different temperatures with coverage show that two kinds of V_{Zn} -related defects (namely V_{Zn-1} and V_{Zn-2}) having different microstructures are present in the undoped PLD grown samples [6,7]. For the undoped sample grown at $T_{sub}=300\text{ }^{\circ}\text{C}$ and $P(O_2)=0\text{ Pa}$, V_{Zn-1} is the only V_{Zn} -related defect existing in the as-grown sample. V_{Zn-1} disappears at the annealing temperature of 900°C , and a new single V_{Zn} -related defect (i.e. V_{Zn-2}) is identified. The introduction of the single type of V_{Zn} -related defect V_{Zn-2} is also observed in all the samples grown with different T_{sub} and $P(O_2)$. The thermal introduction of V_{Zn-2} at $900\text{ }^{\circ}\text{C}$ well correlates with the introductions of the GL-2.47eV defect emission and the DAP/FA NBE emission in the PL study. Furthermore the photon energy of the GL-2.47eV matches with the transition from the conduction band minimum (CBM) to a state at $E_V+0.93\text{ eV}$, and that of the DAP/FA emission at 3.23 eV is associated with the acceptor at $E_V+0.19\text{ eV}$ (see figure 3(b)). These two acceptor levels coincide well with the $\varepsilon(0/-)=0.18\text{ eV}$ and $\varepsilon(-/2-)=0.87\text{ eV}$ of the doubly ionized acceptor V_{Zn} as obtained by the first principal calculation [11]. The origins of the GL-2.47eV and the 3.229 eV DAP/FA emissions are thus attributed to the V_{Zn} defect.

The Doppler broadening spectrum reflects the electronic momentum distribution ($p_z=2\Delta E/c$, where ΔE is the energy away from the 511 keV annihilation peak) at the positron annihilation site [9,10]. The high momentum part of the Doppler broadening spectrum involves the annihilation between the positron and the high

momentum core electrons. Thus the characteristic structure of the high momentum Doppler broadening spectrum (~ 10 keV away from the 511 keV annihilation peak) is related to the chemical element around the annihilation site [9,10]. However, the high momentum part of the Doppler broadening spectrum is usually shielded behind the background in the conventional single detector Doppler broadening study. Employing the coincidence setup with two detectors, the coincidence Doppler broadening (CDB) study is performed to study the different Zn-vacancy related defects presence in the undoped ZnO samples annealed at 900 °C with and without coverage, and the Cu-doped ZnO sample. As compared to the S and W parameter study, CDB has the advantage of offering the electronic momentum distribution around the Zn-vacancy related defect, which is indeed the figure print of the defect.

Their ratio curves obtained by making reference to the CDB spectrum of the as-grown undoped ZnO film grown at $T_{\text{sub}}=300$ °C and $P(\text{O}_2)=0$ Pa are shown in figure 4. This implies that the figure print ratio curve of the as-grown sample (i.e. VZn-1) is the function of unity. The ratio curve of the as-grown Cu-doped ZnO samples is shown in figure 4. A negative peak is found at $p_L \sim 14 \times 10^{-3} m_0 c$. The ratio curve of a pure Cu metal sample is also shown figure 4, which shows the similar negative peak nature as that of the Cu-doped ZnO sample. It thus reveals the presence of the Cu decorated V_{Zn} complex in the as-grown Cu-doped ZnO sample. The ratio curve of the undoped ZnO sample annealed at 900 °C with coverage (i.e. VZn-2) is shown in figure 4. It is distinct from that of VZn-1. This result agrees well with that obtained from the S-W parameter study as discussed in the previous paragraph. VZn-2 has the electronic momentum distribution similar to that of VZn-1 with $p_L < 20 \times 10^{-3} m_0 c$, and decreases with increasing p_L with $20 \times 10^{-3} m_0 c < p_L < 30 \times 10^{-3} m_0 c$. The ratio curve of the undoped ZnO sample annealed at 900 °C without coverage

shows very similar nature to that of VZn-2. It is thus concluded the Zn-vacancy related defects found in the undoped ZnO samples annealed at 900 °C with and without coverage are the same and have the same microstructure, although the Zn out-diffusion in the sample annealed with cover is more extensive.

In the present study, the GL-2.47eV defect emission as found in the undoped PLD grown samples annealed at 900 °C with cover is attributed to the V_{Zn} . However it does not imply that all the green luminescence observed in other samples grown with different methods and treated with different post-growth annealing originate from V_{Zn} . For the present systematic study on PLD grown ZnO, for samples annealed at temperatures lower than 900°C we have observed defect emissions having different shapes and peaking from 2.2 eV to 2.5 eV, depending on the initial growth conditions and the annealing temperature. The variation of the shape and peak position is associated with changes of the relative concentrations of defects emitting different photon energies in the different samples. As the annealing temperature increases to 900 °C, the GL-2.47eV emission is observed in all the samples, irrespective of the initial growth conditions, implying that only the V_{Zn} remains contributing for the defect emission after the 900 °C annealing treatment. Two kinds of green luminescences peaking at 2.30 eV and 2.53 eV observed by Ton-That et al [12] have been a in O-rich and Zn-rich samples and are ascribed to V_{Zn} and V_O - related defects respectively. Lv and Li [13] reported that the shape and the peak position of the green luminescence observed depended on the abundance of the V_O , V_{Zn} and O_i defects. This explains the difficulty and controversy of using the defect emission as a probe for the type of defect in ZnO, as the broad defect emission may originate from more than one type of defect. Care is also needed while concluding on the origin of the defect emission only by comparing the peak position. We have collected LT PL

spectra of the same undoped sample annealed at 900 °C using two different gratings, with blazes of 250 nm and 500 nm. The peaks of the green luminescence are different, namely at 2.47 eV and 2.55 eV for the gratings with the blaze of 500 nm and 250 nm respectively.

In the present study, V_{Zn} -related defects are present in the ZnO films grown on c-plane sapphire after annealing at 900 °C. However, previous PAS studies on bulk ZnO single crystal commonly reported on annealing temperatures lower than 400 °C [14-16]. The presence of V_{Zn} -related defects in ZnO films grown on sapphire after annealing at 900 °C is probably related to the thermally induced Zn out-diffusion from the ZnO which would inevitably create V_{Zn} -related defects.

Zn out-diffusion from the ZnO film is observed in the present ZnO/sapphire interface at the annealing temperature of 750 °C. Wang et al [17] also observes Zn out-diffusion from the ZnO films in ZnO/sapphire and ZnO/MgO structure upon annealing at 500 °C using SIMS, accompanied by the formation of electrically active deep traps (as revealed by deep level transient spectroscopy DLTS), the enhancement of the green luminescence, and the suppression of the NBE emission. These results show that the ZnO/sapphire and ZnO/MgO interfaces are relatively thermally unstable. Zn out-diffusion would create V_{Zn} deep acceptors which would compensate the free carriers. Caution thus needs to be taken on the interface, and in particular for the case of fabricating p-type ZnO material.

CONCLUSION

The thermal stability of the film-substrate interface and defects in PLD grown undoped and Cu-doped ZnO films grown on c-plane sapphire were studied. Two kinds of green defect emissions were identified in the undoped and the Cu-doped

samples upon annealing. Three kinds of Zn-vacancy related defects were identified in the samples depending on the annealing treatment and the Cu-doping. The thermal stability of the ZnO/sapphire interface is dependent on whether the surface of the ZnO sample is covered during annealing. The green luminescence peaking at 2.47 eV and the NBE emission at 3.23 eV introduced after the 900 °C annealing are associated with V_{Zn} .

ACKNOWLEDGEMENT

The present study is financially supported by the HKSAR RGC under the scheme of GRF (project no. 7036/12P), as well as the University Development Fund and the Small Project Grant from The University of Hong Kong.

Manuscript submitted to Physica B for the Proc. SCAPM 2015

REFERENCES

- [1] Ü. Özgür, Ya. I. Alivov, C. Liu, A. Teke, M. A. Reshchikov, S. Doğan, V. Avrutin, S.-J. Cho and H. Morkoç, J. Appl. Phys. **98**, 041301 (2005).
- [2] S. C. Su, H. Zhu, L. X. Zhang, M. He, L. Z. Zhao, S. F. Yu, J. N. Wang, and F. C. C. Ling, Appl. Phys. Lett. **103**, 131104 (2013).
- [3] D. C. Look, Phys. Stat. Sol. B **241**, 624 (2004).
- [4] V. Avrutin, D. J. Silversmith, and H. Morkoç, Proc. IEEE **98**, 1269 (2010).
- [5] M. D. McCluskey and S. J. Jokeia, J. Appl. Phys. **106**, 071101 (2009).
- [6] Z. L. Wang, S. C. Su, F. C. C. Ling, W. Anwand, and A. Wagner, J. Appl. Phys. **116**, 033508 (2014).
- [7] Z. L. Wang, S. C. Su, M. Younas, F. C. C. Ling, W. Anwand, and A. Wagner, RSC Advances **5**, 12530 (2015).
- [8] R. Dingle, Phys. Rev. Lett. **23**, 579 (1969).
- [9] R. Krause-Rehburg, and H. S. Leipner, *Positron Annihilation in Semiconductors-Defects Studies* (Springer, Berlin, 1999).
- [10] F. Tuomisto, and I. Makkonen, Rev. Mod. Phys. **85**, 1583 (2013).
- [11] A. Janotti and C. Van de Walle, Phys. Rev. B **76**, 165202 (2007).
- [12] C. Ton-That, L. Weston, and M. R. Phillips, Phys. Rev. B **86**, 115205 (2012).
- [13] J. P. Lv and C. D. Li, Appl. Phys. Lett. **103**, 232114 (2013).
- [14] F. Tuomisto, K. Saarinen, D. C. Look, and G. C. Farlow, Phys. Rev. B **72**, 085206 (2005).

- [15] Z. Q. Chen, S. J. Wang, M. Maekawa, A. Kawasuso, H. Naramoto, X. L. Yuan, and T. Sekiguchi, Phys. Rev. B **75**, 245206 (2007).
- [16] L. W. Lu, C. K. So, C. Y. Zhu, C. J. Li, S. Fung, G. Brauer, W. Anwand, W. Skorupa, and C. C. Ling, Semicond. Sci. Technol. **23**, 095028 (2008).
- [17] R. S. Wang, Q. L. Gu, C. C. Ling, and H. C. Ong, Appl. Phys. Lett. **92**, 042105 (2008).

Manuscript submitted to Physica B for the Proc. SCAPM 2015

CAPTIONS

Figure 1 (a) The cross-sectional HRTEM image at the film/substrate interface (dark arrows) for the undoped ZnO/sapphire sample annealed at 750°C without covering the surface. The inset shows the electron diffraction pattern from the film-substrate interface; (b) The cross-sectional HRTEM image at the film/substrate interface for the undoped ZnO/sapphire sample annealed at 750°C with covering the surface. The corresponding diffraction pattern from film-substrate interface is presented in the inset. The undoped samples are grown at $T_{\text{sub}}=600$ °C without oxygen.

Figure 2 (a) The SIMS depth profiles of Al and Zn for the undoped ZnO/sapphire sample annealed at 900 °C with the surface covered. The shaded region marks for the width for the Zn intensity decays to 10%; (b) The SIMS depth of Al and Zn for the undoped sample annealed at 900 °C without the surface cover. The undoped sample is grown at the substrate temperature of 600 °C without oxygen.

Figure 3 (a) The defect emissions of the PL spectra taken at the temperature of 10 K for the undoped ZnO/sapphire film annealed at 900 °C with and without coverage, and the Cu-doped ZnO/sapphire film upon the annealing of 900 °C with cover. The insert shows the normalized defect emission taken at the temperature of 10 K for the different undoped ZnO/sapphire films grown at $T_{\text{sub}}/P(\text{O}_2)$ equal to 300°C/0 Pa, 300 °C/5 Pa, 600 °C/0 Pa, and 600 °C/5 Pa annealed at 900 °C with coverage; (b) The NBE emission of the undoped ZnO sample annealed at 900 °C taken at temperatures from 10 K to 150 K. The D^0X and TES are red-shifted while the DAP/FA are blue-shifted with the increasing temperature. The insert shows the energy scheme of the transitions leading to the DAP/FA and the green luminescence at 2.47 eV. The $\varepsilon(0/-)$ and $\varepsilon(-/2-)$ are the two acceptor levels of V_{Zn} .

Figure 4 The ratio curves for the CDB spectra for the as-grown Cu-doped ZnO sample, the pure Cu metal, and the undoped ZnO samples annealed at 900 °C with

and without coverage. The ratio curves are plotted with reference to the as-grown undoped ZnO sample grown without oxygen.

Manuscript submitted to Physica B for the Proc. SCAPM 2015

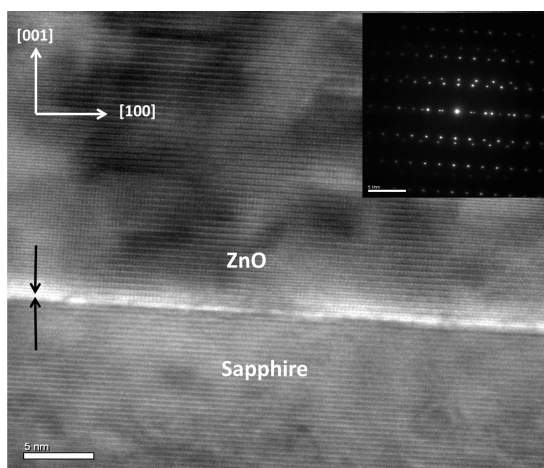


Figure 1(a)

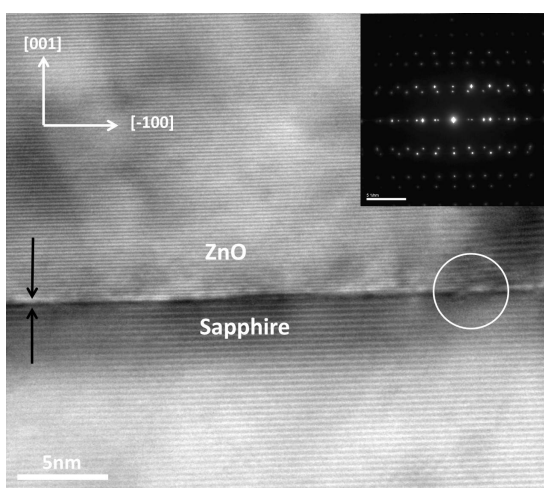


Figure 1(b)

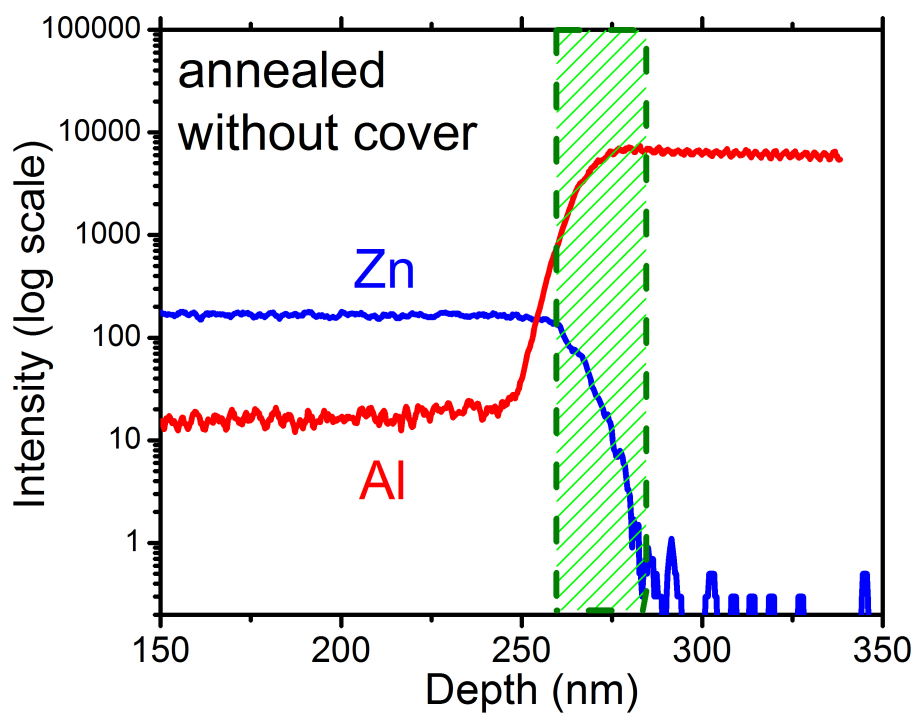


Figure 2 (a)

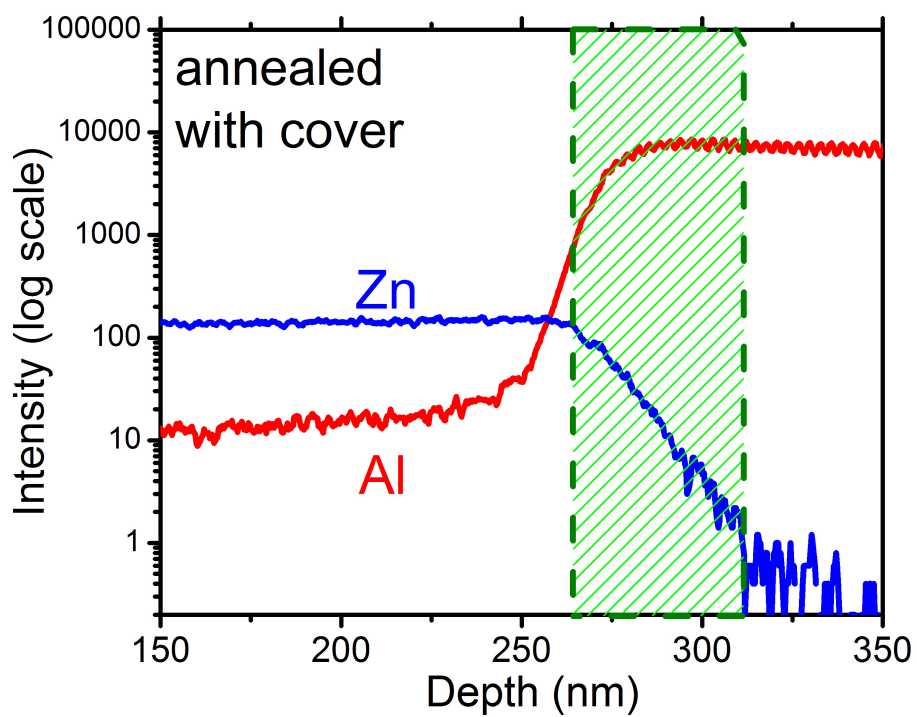


Figure 2(b)

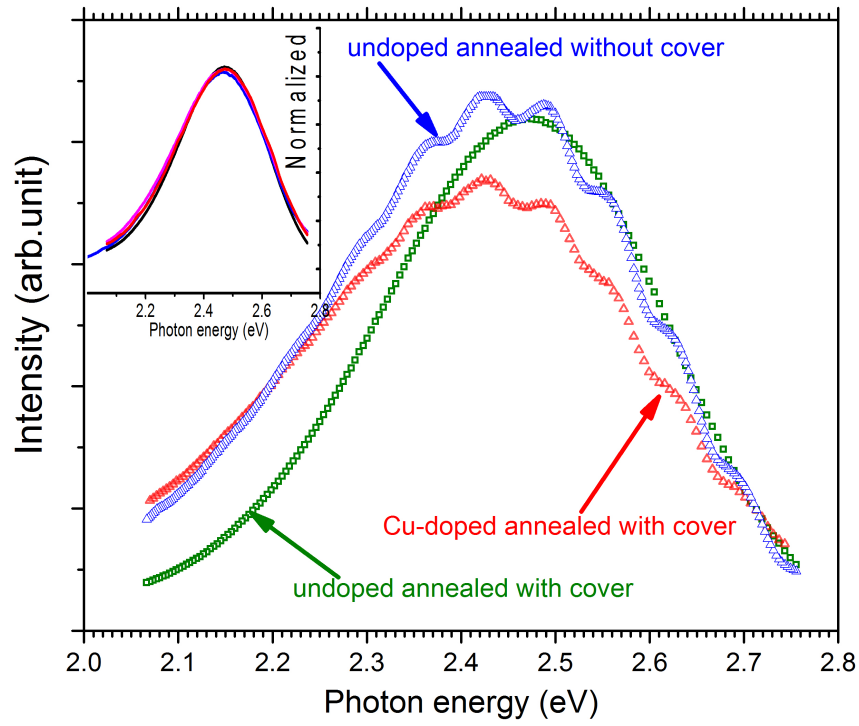


Figure 3(a)

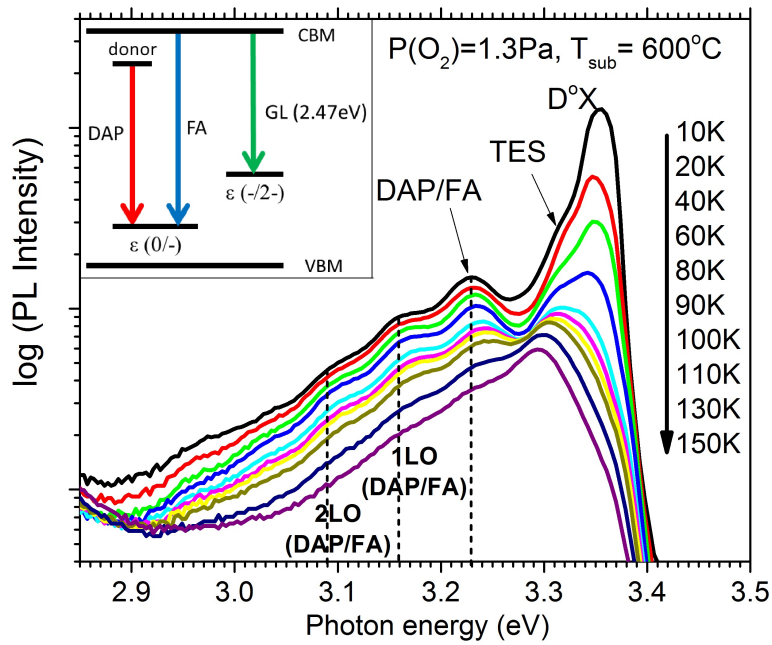


Figure 3(b)

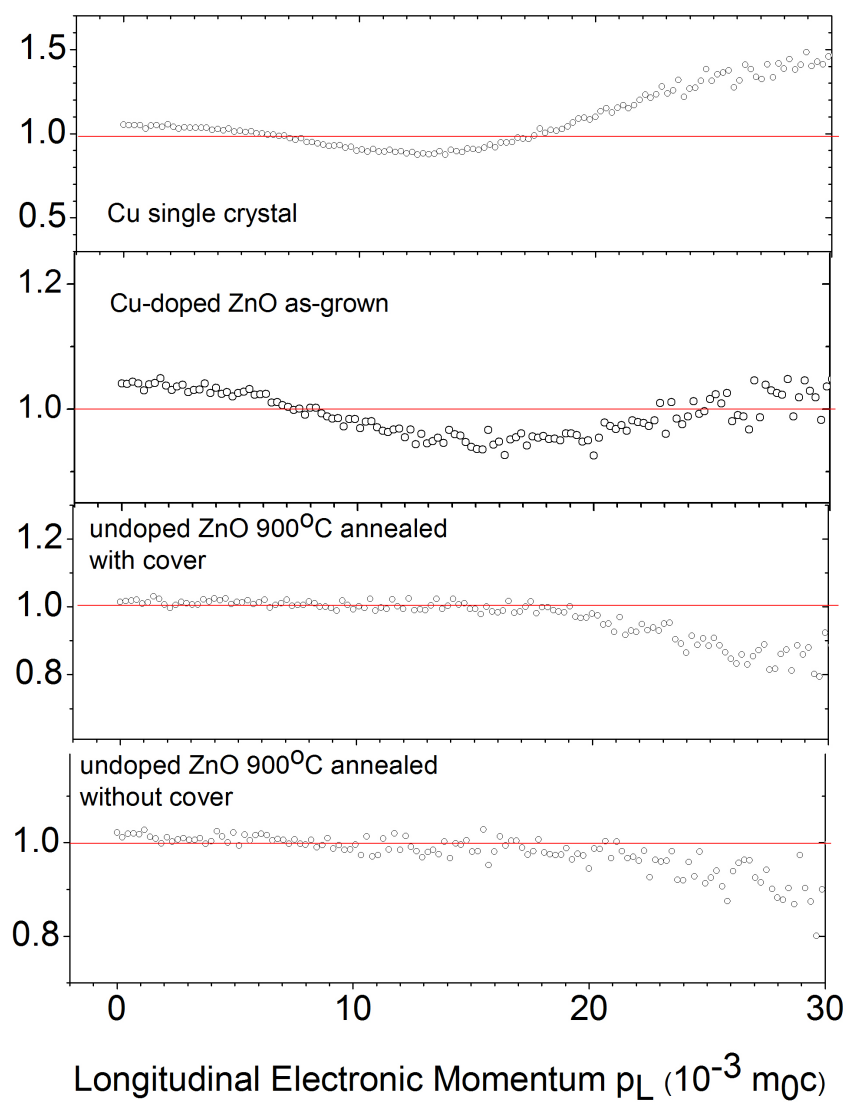


Figure 4